The holobiont's extracellular microbiome modulates the adaptation of an intracellular endosymbiont

Madangchanok Imchen[1], Rupinder Kaur[1], Angelina McGarry[1], and Seth R. Bordenstein[1]*

[1]Departments of Biology and Entomology, One Heath Microbiome Center, Huck Institutes of the Life Sciences, The Pennsylvania State University, USA

* Corresponding author
E-mail: srb6251@psu.edu

Keywords: cytoplasmic incompatibility, microbiome, intracellular bacteria, symbiosis, *Drosophila melanogaster*.

Abstract

Animal holobionts contain two broad classes of microorganisms, intra- and extracellular microbes, that are largely studied in symbiotic siloes. Here we demonstrate the impact of the extracellular gut microbiome on an intracellular reproductive endosymbiont using the *Drosophila melanogaster* holobiont and its endosymbiont *Wolbachia* that adaptively cause a paternal-effect lethality of embryos termed cytoplasmic incompatibility (CI). We report the endosymbiont's adaptation is not only self-sufficient but stronger in a host without an extracellular microbiome. Indeed, host transcripts associated with the CI adaptation are enhanced, while cell biological hallmarks exhibit complex quantitative and qualitative differences in microbiome-free hosts. Decreases in the gut bacteria *Lactobacillus* specifically link with high penetrance of the CI adaptation. Notably, both the extracellular microbiome and endosymbiont harbor markedly higher cellular densities in a complete holobiont setting than when either constituent is reared alone. Altogether, this study uncovers a novel interaction whereby the extracellular microbiome modulates the phenotype of an intracellular endosymbiont, revealing intricate symbiotic networks within the holobiont.

Introduction

Animal and plant holobionts contain a consortium of microorganisms spanning intracellular endosymbionts and extracellular microbes with varying degrees of interdependencies [1,2]. The co-existence of these endosymbionts and extracellular microbes with different lifestyles and functions can impact each other in competitive or collaborative ways [3], potentially generating trade-offs and synergies across symbiotic types and host anatomical sites throughout a host's lifespan. The net outcome of such multipartite interactions may leave symbiotic ripple effects in a holobiont.

Challenges to assessing the specific impacts of the extracellular microbiome on endosymbioses are two-fold. First, microbiome elimination methods are often indiscriminate to the extracellular and intracellular microbiome, and second, most endosymbionts cannot be cultured outside of the host cell [4]. Here, we overcome these factors using *Drosophila melanogaster* that can be reared without its simple extracellular gut microbiome [5] while maintaining the vertically-inherited, intracellular endosymbiont. This is accomplished by dechorionation of the fertilized eggshell layer that removes the extracellular microbiome while maintaining the internal endosymbiont.

The α-proteobacterium *Wolbachia* is an archetypical intracellular reproductive endosymbiont of *D. melanogaster* and one of the most widespread, maternally-inherited, bacteria in multicellular eukaryotes [6]. *Wolbachia* are widely known for their diverse effects on manipulating host reproductive biology, in particular cytoplasmic incompatibility (CI), whereby crosses between symbiotic males and aposymbiotic females result in embryonic death [7–11]. Notably, the embryos are rescued if the females harbor *Wolbachia*. Thus, CI is a selfish

evolutionary adaptation that enhances the relative fitness of symbiont-transmitting females and thus *Wolbachia*'s spread through host populations [8].

Here, we leveraged the *D. melanogaster* holobiont to disentangle the impact of the extracellular microbiome on an endosymbiont's adaptation, densities, and fitness impacts on the host. We address three central questions: Can an intracellular endosymbiont operate independently of an animal's extracellular microbiome? If so, does the endosymbiont benefit from this altered holobiont? What alterations in host and endosymbiont biology manifest in a strict, single-pair, animal-microbe endosymbiosis relative to the complete holobiont setting?

Results

We generated *D. melanogaster* lines both with and without *Wolbachia* and the extracellular microbiome (e.g., gut microbiome). *w*Mel *Wolbachia* is a member of the fly microbiome, yet for simplicity and the purposes of the paper, we separately define the conventional microbiome as the community of extracellular microbes and the endosymbiont *Wolbachia* as the intracellular microbe. Thus, we adhere to the typical nomenclature system of conventional (CV) and germ-free (GF) lines, both with *Wolbachia* (CV+ and GF+) and without it (CV- and GF-). We confirmed *Wolbachia* infection status by PCR (Fig S1) and GF status of *Wolbachia*-infected and uninfected flies by plating whole fly homogenates of GF reared flies (see methods) and demonstrating no colony-forming units (CFUs) (Fig S2).

Absence of an extracellular microbiome promotes an endosymbiotic adaptation and host gene activation

80 To determine whether or not the CI adaptation is contingent on the extracellular fly
81 microbiome, we set up single-pair matings of <1-day-old, CI-inducing males carrying *Wolbachia*
82 (CV+ and GF+) and aposymbiotic females lacking *Wolbachia* (CV- and GF-). While CI levels by
83 CV+ males were moderate and typical for *w*Mel CI (median embryonic hatch rate = 36.17%), GF+
84 males notably induced 2.6-fold stronger CI (median = 13.66%) (Fig 1a). This strengthening of
85 embryonic lethality was fully rescued by CV+ females, demonstrating it was bona fide CI and not
86 an artifactual host sterility (Fig 1a).

87 The cell biological hallmarks of CI induction in male testes include abnormal histone
88 retention and decreased protamine deposition in developing sperm [7]. To evaluate if these gametic
89 modifications occur in GF+ males that express stronger CI, we first performed RNA-seq on late
90 male pupae when the histone-to-protamine transition commences in *D. melanogaster* [12,13]. The
91 core nucleosome structure is composed of H2A, H2B, H3, and H4 classes of histone proteins [1].
92 The expression of corresponding *His2Av*, *His2B*, *His3.3A*, *His3.3B*, and *His4r* genes were
93 upregulated in GF+ pupae compared to CV+ (Table S2). In *Drosophila* spermiogenesis, H3.3
94 variant along with the bulk histones are removed in the early canoe stage during the histone-to-
95 protamine transition [14]. Notably, expression of the *His3.3B* gene encoding the H3.3 class of
96 histone protein [15] was significantly upregulated in GF+ males relative to CV+ males (fold
97 change = 1.82, Log2FC= 0.87, $p < 0.05$) (Fig 1b). Moreover, expression of histone
98 methyltransferase 4-20 (*Hmt4-20*) that marks DNA for damage repair [16] was also significantly
99 upregulated (fold change = 1.82, Log2FC= 0.86), suggesting the host is attempting to keep up with
100 the elevated DNA damage in developing CI sperm [2]. Furthermore, comparative analysis indicated
101 that four of the five significant differentially-expressed genes involved in histone functions had an

102 enhanced relative gene expression ratio in GF+ vs. CV+ compared to GF- vs. CV-, suggesting that
103 *Wolbachia* can drive enhanced expression of CI-related cellular features in the GF+ state.
104 Further, there are four well-characterized protamine and protamine-like genes essential for
105 *Drosophila* mature sperm formation [17,18]. As expected for the CI-induced depletion of
106 protamine abundance in sperm, *ProtB*, *Prtl99C*, and *Mst77F* were significantly downregulated in
107 GF+ vs. CV+ male pupae (Fig 1b), and *ProtA* expression trended non-significantly lower (Table
108 S2). Consistent with the histone gene expression pattern above and protamine depletion as causal
109 to CI, three out of the four significant protamine genes had weakened transcription in GF+/CV+
110 relative to GF-/CV-.
111 Many male-specific transcripts involved in secretory proteins and spermatid maturation,
112 e.g., *Mst57Da*, *Mst57Db*, and *Mst57Dc*, were also significantly downregulated in GF+ compared
113 to CV+, collectively suggesting that CI-*Wolbachia* generally weaken gene expression of sperm-
114 associated proteins. Consistent with the aforementioned gene expression trends for CI-related gene
115 functions, 13 of the 15 significant *Mst* genes had a more pronounced fold change in GF+/CV+
116 relative to GF-/CV-.
117 Overall, the results specify that transcriptomic changes of key cell biological pathways in
118 CI links with augmented CI penetrance in flies that lack an extracellular microbiome. Interestingly,
119 GF- males without *Wolbachia* appear transcriptionally primed to express CI, but to a lesser degree
120 than when *Wolbachia* occur. This observation suggests moderate enhancements of transcriptome
121 changes coupled with expression of the CI genes in GF+ males may tip the cellular balance towards
122 enhanced CI expression.
123

124 **Fig 1. CI penetrance is stronger in germ-free males and associates with gene expression**
125 **variation in histone, protamine, and male-specific transcripts.** (a) Germ-free males with
126 *Wolbachia* (GF+) induce significantly higher CI or incompatibility (purple) than conventional
127 (CV+) males. CI is a metric for embryonic viability that is measured by the percentage of embryos
128 that hatch into larvae. Compatible crosses (grey bars) with normal embryonic hatching percentages
129 are controls that express either no CI or rescue of CI. P-values were calculated based on a Kruskal-
130 Wallis test followed by Benjamini, Krieger, and Yekutieli multiple correction test. The vertical
131 bars represent the median value, and the error bars represent the 95% confidence interval. (b)
132 Comparative transcriptomic analysis of GF+ vs. CV+ male pupae (bars filled with black dots) and
133 GF- vs. CV- male pupae (bars without black dots) revealed many significant Differentially
134 Expressed Genes, which were further screened to 24 genes that represented histone, protamine,
135 and male-specific transcripts (MSTs). Significant differences are highlighted with a red colored
136 asterisk (*). Notably, the histone-related genes genes (blue) were upregulated, while protamine
137 (grey) and MST (yellow) genes were downregulated. Log2 fold change was calculated using
138 DESeq2, and its default parameters; Walt test and Benjamini-Hochberg procedure were used to
139 calculate p and adjusted p-values. The asterisk *, **, and *** represent adjusted p-values less than
140 0.05, 0.005, and 0.0005, respectively.
141

142 Cell biological modifications of host chromatin integrity occur in flies
143 lacking an extracellular microbiome

144 To test if CI-related host nucleoprotein signatures occur in GF+ flies, we next compared
145 histone abundance in spermatids and protamine deficiency in matured sperms of GF+ males.

146 Immunostaining <8-hour-old testes of virgin CI-inducing GF+ and CV+ males using a core histone
147 antibody showed significant histone retention in late canoe spermatid bundles, as expected
148 compared to GF- and CV-, respectively. The level of histone retention between the two groups
149 varied, with GF+ canoe spermatids exhibiting a median of 15.48% histone retention compared to
150 0% for GF- males (Fig 2a,b), and CV+ testes showing 57.14% histone retention compared to
151 12.14% for CV- males. As such, quantitative differences in histone retention are enhanced in CV+
152 males, while qualitative differences are larger in GF+ males. These differences are discussed
153 below.

154 Finally, cytochemical staining of mature sperm from <1-day-old virgin males with the
155 chromomycin A3 (CMA3) stain that binds to DNA regions devoid of protamines specified the
156 expected protamine deficiency is 1.45-fold elevated in mature sperm of GF+ compared to GF-
157 males (Fig 2b,d). These results are consistent with *Wolbachia* in a GF+ host modulating the
158 protamine deposition onto mature sperm in a slightly enhanced manner relative to the deficiency
159 of a 1.3 fold difference in CV+ vs. CV- males (Fig 2). Previous work demonstrated that enhanced
160 protamine deficiency is causal to increases in CI penetrance [3].

161

162 **Fig 2. CI defects in the histone-to-protamine transition occur in germ-free and conventional**
163 **males.** (a) Testes (N = ~10) from <8-hour-old virgin males of GF-, GF+, CV-, and CV+ lines were
164 dissected and immunostained to visualize and quantify histone abundance (magenta) in late-canoe
165 elongating spermatids. DAPI stain (grey) was used to label spermatid nuclei. (b) Total spermatid
166 bundles with DAPI signals and those with retained histones were manually counted and graphed.
167 Signal intensity in each sperm nucleus head was quantified in ImageJ and graphed. GF+ and CV+

168 males show a significantly higher number of spermatid bundles with retained histones compared
169 to their negative counterparts GF- and CV-, respectively. (c) Fully mature sperm were extracted
170 from <1 day-old virgin males of GF-, GF+, CV-, and CV+ lines and stained with fluorescent
171 CMA3 (green) for detection of protamine deficiency. (d) Quantification of the signal intensity
172 using ImageJ shows that GF+ and CV+ sperm have enhanced CMA3 intensity, consistent with
173 protamine deficiency levels compared to GF- and CV- negative controls, respectively. Vertical
174 bars represent the median, and error bars represent the standard deviation. P-values in the bracket
175 are calculated using the Mann-Whitney U test and the p-values outside of the bracket are calculated
176 using the Kruskal-Wallis test.
177

178 Endosymbiont density decreases in a microbiome-free host

179 Higher CI strength can depend on several, common factors including but not limited to an
180 increased density of *Wolbachia* [19], increased expression of *cif* genes [20], and/or reduced host
181 resistance to CI [21]. We measured relative *Wolbachia* density (*groEL)* compared to *D.*
182 *melanogaster* housekeeping gene *rp49*. Interestingly, *Wolbachia* density was reduced 4.58-fold in
183 strong CI-inducing GF+ males relative to CV+ males expressing moderate CI (Fig 3a). Moreover,
184 the relative expression of CI-associated genes *cifA* and *cifB* compared to *Wolbachia groEL* was
185 similar between CV+ and GF+ in adults (Fig 3b, c) and larvae (Fig S3), indicating that relative *cif*
186 gene transcription is independent of the *Wolbachia* density decline and loss of the extracellular
187 microbiome. Taken together, we conclude that GF+ males experience stronger CI not because they
188 experience an acute increase in symbiont number or gene expression (e.g., exemplary of a hyper-
189 pathogenic state), but instead because the hosts are physiologically more susceptible to the same

190 CI-induced modifications induced with lower *Wolbachia* densities in a microbiome-free or
191 conventional state.
192
193 **Fig 3. *Wolbachia* density is markedly lower and relative *cif* gene expression is equal in a**
194 **germ-free host.** (a) *Wolbachia* density was determined in CV+ and GF+ adult males by
195 quantifying single copy *Wolbachia* housekeeping gene *groEL* relative to *D. melanogaster*
196 housekeeping gene *rp49*. *Wolbachia* density was significantly lower in the GF+. (b) *cifA* and (c)
197 *cifB* gene expression were quantified by the ratio of cDNA from single copy *cifs* relative to the
198 *Wolbachia* housekeeping gene *groEL*. Gene expression was similar between GF+ and CV+,
199 indicating higher CI penetrance is not attributable to *cif* gene expression. The p-values are shown
200 for the non-parametric Kolmogorov-Smirnov test of equal distributions and Mann-Whitney U test
201 of population differences in the bracket.
202

203 Endosymbiont promotes extracellular microbiome growth

204 The microbiome of *D. melanogaster* is predominantly composed of 5 core culturable
205 species from the genera Lactobacillus and Acetobacter (Ludington & Ja, 2020). To assess if there
206 are microbiome abundance differences between conventionally reared flies with (CV+) and
207 without *Wolbachia* (CV-) that associated with CI penetrance variation, we plated whole adult male
208 homogenates onto *Lactobacillus* (MRS agar plates) and *Acetobacter* spp. (MYPL agar plates)
209 selective media (Aranda-Díaz et al., 2020) and counted the number of colony forming units
210 (CFUs) after 48 hours. CFUs of *Acetobacter* and *Lactobacillus* species in CV+ were notably 7.07-
211 and 9.78-fold higher compared to CV- (Fig 4a). Thus, an intact holobiont with the endosymbiont
212 contains nearly an order of magnitude more cells of the extracellular microbiome. Moreover, there

213 was a positive correlation between the overall CFUs of *Acetobacter* and *Lactobacillus* (Fig 4b)
214 that validated previous reports [22,23]. In parallel, we demonstrated no CFUs from negative-
215 control homogenates from GF+ and GF- males, as expected (Fig S2). Taken together with data in
216 Fig 3a, an intact holobiont contains markedly more cells of both the extracellular microbiome and
217 *Wolbachia* endosymbiont.

218 Based on this observation, we next tested if the abundance of cells from the extracellular
219 microbiome link with the penetrance of CI. Since GF+ males without a gut microbiome yield
220 significantly lower levels of embryos hatching and thus higher CI, we hypothesized that variation
221 in CI penetrance in CV+ males is associated with variation in the abundance of some gut microbes.
222 Indeed, there is a strong positive correlation between embryonic hatch rates from CI-causing CV+
223 males and the CFU count of *Lactobacillus* spp. (Fig 4d). Conversely, there is no association with
224 the CFU counts of *Acetobacter* spp. (Fig 4e), specifying then that higher *Lactobacillus* spp.
225 abundance links with reduced CI penetrance.

226

227 **Fig 4. Holobionts with *Wolbachia* have higher colony forming units (CFUs) of gut bacteria,**
228 **of which *Lactobacillus* negatively associates with CI strength.** (a) Homogenates of less than
229 one day old CV- (white circles) and CV+ males (orange circles) (N=5) in triplicates were spread
230 on MRS and MYPL plates. (b) *Wolbachia* infection (CV+) significantly increased the CFU load
231 of *Acetobacter spp*. and *Lactobacillus spp*., suggesting a positive interaction between the
232 endosymbiont and the microbiome. The p-values are calculated with a Mann-Whitney U test. (c)
233 The CFU of *Acetobacter* spp. and *Lactobacillus* spp. in CV- (data points filled in white) and CV+
234 (data points with filled in orange color) males have a significant positive correlation. (d) The CFU
235 of *Lactobacillus* spp. in CV+ males showed a significant correlation with the embryonic CI hatch

236 rate (HR) levels from the cross ♂CV+ x ♀wMel-. (e) Conversely, the CFU of *Acetobacter* spp. in
237 CV+ males did not exhibit a significant correlation with the hatch rate.
238

239 The extracellular microbiome and endosymbiont independently
240 impact survival across development

241 Next, we examined the impact of the extracellular microbiome and endosymbiont on host
242 fitness and development across various life stages. We reared flies with (CV+ and GF+) and
243 without *Wolbachia* (CV- and GF-), and we measured the survival of the fly through metamorphosis
244 from embryo-to-larvae, larvae-to-pupae, and pupae-to-adults. GF+ flies with only *Wolbachia* had
245 a significantly higher embryonic hatch rate to larvae (71.43%) than GF- flies without *Wolbachia*
246 (66.95%, Fig 5a). CV+ flies similarly had higher survival (87%) than CV- flies lacking *Wolbachia*
247 (82%). Thus, the presence of *Wolbachia* generally enhanced egg-to-larvae survivability to a
248 modest degree. However, CV+ embryos exhibited higher embryo-to-larval hatching (87%) than
249 GF+ (71.43%), suggesting that a complete microbiome is beneficial for embryo-to-larvae
250 survivability. Thus, holobiont development with *Wolbachia* is optimized at this stage. From
251 larval-to-pupal (L-P) and pupal-to-adult (P-A) development stages, *Wolbachia* universally reduced
252 survival compared to their negative control counterparts, specifying a modest, negative fitness cost
253 at the larval stage onwards (4-13% reduction in survival, Fig 5b,c). Nonetheless, holobiont
254 survival was higher during the L-P stage (CV+ vs GF+, 11.67% increase, Fig 5b), indicating a
255 compensatory effect of the extracellular microbiome. Altogether, these findings specify that
256 *Wolbachia*'s impacts on survival (beneficial to embryonic development, but harmful to subsequent
257 stages) are independent of those of the extracellular microbiome.

258

259 **Fig 5. The fitness impacts of *Wolbachia* are independent of the extracellular microbiome and**
260 **stage-dependent on metamorphosis**. (a) The extracellular microbiome and *Wolbachia* exert
261 independent and positive effects on embryo-to-larval survival, as calcuated by the number of
262 surving larvae divided by the number of emryos laid. (b) The extracellular microbiome is
263 beneficial to larval-to-pupal survival, while *Wolbachia* imposes a fitness cost in a microbiome-
264 independent manner. (c) Similarly, *Wolbachia* lower pupal-to-adult survival percentage in a
265 microbiome-independent manner. Each circle represents a family, and color denotes genotype
266 status: orange bar (CV), blue bar (GF), open circle (no *Wolbachia*), and filled cirlce (*Wolbachia*).
267 The p-values are shown were calculated with Kruskal-Wallis test followed by Benjamini, Krieger,
268 and Yekutieli multiple correction test.

269

270 Discussion

271 How the extracellular microbiome influences intracellular symbiont biology is poorly
272 known. Here we addressed this knowledge gap in a model system by examining the impacts of *D.*
273 *melanogaster*'s extracellular microbiome on an intracellular endosymbiont and its CI adaptation,
274 which manifests as a paternal-effect embryonic lethality when a *Wolbachia*-symbiotic male mates
275 with an aposymbiotic female. We report five specific findings: (i) CI penetrance is stronger in GF+
276 *D. melanogaster* lacking an extracellular microbiome. (ii) CI strength in GF+ vs. CV+ males is
277 independent of *Wolbachia* density and CI gene expression. (iii) transcriptomic reveal moderate
278 upregulation of histone genes and downregulation of protamine and testes-specific genes that are
279 consistent with known CI functions [7,24]. (iv) cell biological analyses in male reproduction

280 uncover complex quantitative and qualitative differences in histone retention and a slightly
281 increased protamine deficiency in germ-free males, as expected for elevated CI levels [3]. (v)
282 Notably, intact holobionts with both *Wolbachia* and gut bacteria have markedly higher microbial
283 densities, and penetrance of CI negatively correlates with a higher abundance of the gut bacteria
284 *Lactobacillus*. (vi) *Wolbachia* generally increase *D. melanogaster* fitness during embryo-to-larval
285 development but exert a fitness cost during larvae-to-pupae and pupa-to-adult development.

286 Influences of the gut microbiome on endosymbiont biology are generally rare because
287 experiments can be complex due to germ-free rearing, and binary interactions are simpler to study
288 than tripartite ones involving multi-species microbial communities. Notably, the gut bacterial
289 genus *Asaia* can impede the vertical transmission of *Wolbachia* in mosquitoes [25]. As such, the
290 nested symbiotic interactions between symbionts in different anatomical sites raise a fresh suite of
291 questions about how mechanistically extracellular and intracellular bacterial interactions impact
292 endosymbiotic functions. These nascent results imply ripple effects of an intricate network of
293 symbiotic interactions within holobionts that are likely to occur in other holobiont systems.

294 CI penetrance in various arthropods was previously known to vary with endosymbiont
295 density, *cif* gene expression, host age, and genetic background, among other traits. [26–30]. Here,
296 we add an unexpected dimension of the gut microbiome to the sources of variation, suggesting
297 heightened sensitivity of the germ-free or microbiome-depleted host to the CI molecular
298 mechanism. Specifically, the load of *Lactobacillus* spp. in males is inversely correlated to the CI
299 strength, the mechanism of which will be subject to future investigations.

300 The impact of the extracellular microbiome and endosymbiont on host fitness across
301 developmental stages revealed an intriguing cascade of intendent fitness impacts of the microbes
302 as well. *Wolbachia* promoted egg-to-larvae survivability, while hindering larval-to-pupal and

303 pupal-to-adult development stages. These effects were microbiome-independent, as evidenced by
304 similar outcomes in GF flies, suggesting that *Wolbachia*'s influences on fly fitness are conditional
305 on developmental stage in a gut microbiome-independent manner, likely due to the endosymbiont
306 residing outside the gut [31].

307 In conclusion, our study disentangled the intricate relationship of the gut microbiome's
308 impact on a key adaptation and replication of a common reproductive endosymbiont. This work
309 aligns with the growing recognition that sources of phenotypic variation, even in presumed simple
310 and binary symbiotic systems such as arthropods and their intracellular *Wolbachia*, can require a
311 broader view of the nested network of symbiotic interactions and functions in holobiont systems.
312 As biology is likely to observe increasing cases of biomolecular interactions of the intracellular
313 microbiome, extracellular microbiome, and the host, there will be new opportunities to understand
314 and apply knowledge that shapes evolutionary symbiotic outcomes and deployment of symbiotic
315 traits for positive outcomes in ecosystem health.
316
317
318
319

Materials and methods

Fly genotype, rearing condition, and food preparation

Drosophila melanogaster y^1w^* (BDSC 1495) lines infected with *Wolbachia* strain *w*Mel were used for all the experiments. *w*Mel uninfected lines were previously established through tetracycline treatment [27]. *Wolbachia* infection status was confirmed through PCR using Wolb_F and Wolb_R3 primers (Table S1). Flies were reared in a 12:12 h light/dark cycle at 25°C and 60-70% relative humidity. The food for CV and GF flies has the same composition but differs in handling – food for GF flies was handled in a sterile condition, and the food for conventionally reared flies was handled in a non-sterile condition. The composition for 1L media consisted of 100gm yeast, 100g dextrose, 40g cornmeal, 7g agar, and 8.8 ml of 10% propionic acid dissolved in ethanol [32].

Rearing of flies to obtain mothers and fathers for hatch rate assay

Adult flies of both sexes were seeded and then cleared on the 4th day. The virgin female offspring (referred to as PGMs – paternal grandmothers) were collected on the 10th to 13th day. The PGM virgins were reared for 4-5 days to ensure virginity and to obtain moderate CI penetrance to test if germ-free treatment yields higher or lower CI penetrance [26]. Virgin PGMs were crossed with males to obtain embryos. In brief, ~30 individuals of 4-7 days old virgin PGMs were allowed to mate with 10 males overnight in a bottle without food secured with a grape plate. The next morning, the grape plate was replaced by a fresh one and incubated for 30 minutes. The grape plate was again replaced by a new one and incubated for 1 hour to obtain 1-hour embryos. In all

341 instances, grape plates were smeared with yeast. The embryos were processed for conventional
342 (CV) and germ-free (GF) treatment. On the 2nd and 9th days after the CV and GF treatments, larvae
343 and pupae survival were counted. On the 10th to 13th day, adult emergence was noticed. Males
344 (referred to as fathers) less than 24 hours old were collected to perform hatch rate assay.
345 Meanwhile, to obtain mothers, adult flies of both sexes were seeded for 4 days and cleared. The 1-
346 3 days old virgin female offspring (referred to as mothers) were collected on the 10th to 13th day.
347

348 **Hatch rate (HR) assay**

349 All crosses were performed with young <1-day-old males [26] and 3 days-old females. The
350 matings were performed in an 8 oz polypropylene bottle and secured with a grape plate. The flies
351 were reared overnight, and the grape plate was replaced by a fresh new grape plate. After 24 hours
352 of rearing, the flies were cleared, and the number of embryos on the grape plate was counted
353 (referred to as the 0-hour count). The embryos were incubated for an additional 36 hours, and the
354 unhatched embryos were counted (referred to as 36-hour count). Any plate with less than 25
355 embryos was discarded. The hatching percentage was determined by calculating the percentage of
356 embryos hatched on the 36-hour count compared to the 0-hour count.
357

358 **Germ-free check and CFU quantification**

359 To score the bacterial CFU in CV flies or to determine the germ-free status in GF flies, less than
360 24 hours old adult male flies (N=5) from each treatment were collected. However, single males
361 from each single-pair cross were collected to assess the bacterial CFU in males from the CI assay.
362 The flies were surface sterilized by washing twice in 70% Ethanol and once in 1x Phosphate-

363 buffered saline (PBS). The surface sterilized flies were crushed with a sterile micro pestle, diluted
364 in 300 uL 1xPBS, and 20 uL was used to spread onto MYPL (*Acetobacter* spp. selective media)
365 media (Aranda-Díaz et al., 2020) and *Lactobacillus* spp. selective media MRS (Sigma, #69964,
366 USA) plates. The MYPL media was composed of 1% D-mannitol (Sigma, #M4125, USA), 1%
367 Yeast extract (VWR, #J850, USA), 0.5% peptone (Thermo Fisher Scientific, # R451102, USA),
368 1% lactic acid (Sigma, #L6661, USA), 0.1% tween 80 (Thermo Fisher Scientific, #278632500,
369 USA), adjusted to pH 7 with NaOH pellets (Spectrum Chemical, #S1301, USA), and 1.5% agar
370 (Sigma, #A1296, USA) was added. The plates were incubated for 48 hours at 30°C and the CFU
371 per fly was quantified using the equation:
372

373 $$CFU\ per\ fly = \frac{Total\ volume\ of\ homogenate\ x\ CFU\ per\ plate}{Total\ flies\ x\ Volume\ plated}$$

374

375 # RNA/DNA isolation for RT/qPCR and transcriptome

376 Less than 6 hours old embryos (N=7), 2 days old larvae (N=7), late-stage pupae (N=1), and less
377 than 24 hours old adults (N=1) in triplicates from each treatment were used to extract RNA and
378 perform RT/qPCR and transcriptome from each treatment in triplicates. Embryos were crushed
379 using a needle, while larvae/pupae/adults were frozen in liquid nitrogen and crushed with a sterile
380 micro pestle. RNA was extracted using 1mL TRI Reagent (Sigma, #93289, USA) and 200 uL
381 chloroform (Sigma, #C2432, USA). Samples were incubated for 3 minutes in an ice block with
382 occasional mixing and centrifuged for 15minutes/12000rpm/4°C. The upper aqueous phase was
383 transferred to an RNase-free microcentrifuge tube containing 500 uL isopropanol & 1 uL
384 glycogen. Samples were incubated for 10 minutes in an ice block with occasional mixing, and

385 centrifuged for 10min/14000rpm/4°C. The supernatant was discarded, and the pellet was washed
386 in 500 uL 75% EtOH followed by centrifugation for 5min/7500rpm/4°C. The pellet was air-dried
387 inside the laminar flow hood at room temperature (RT) until it became translucent. The RNA pellet
388 was resuspended in 30 uL of nuclease-free water and incubated at 55°C for 15 minutes to dissolve
389 the pellet. Any contaminating DNA was eliminated by treating with DNA-free™ DNA Removal
390 Kit (Thermofisher Scientific, #AM9937, USA) as per the manufacturer's instructions. RNA was
391 confirmed DNA-free through negative PCR amplification of *rp49 Drosophila* gene. DNA-free
392 RNA samples were then purified using the ethanol precipitation method (see below) and stored at
393 -80°C until further use. DNA was isolated from the lower non-aqueous layers from the samples
394 used for RNA isolation using Qiagen PureGene Core Kit A kit (Qiagen, #158667, USA) following
395 manufacturer's instructions. However, during the DNA precipitation step we added 500 uL of
396 100% Isopropanol and 1 uL of glycogen to enhance the DNA recovery.
397

398 **Ethanol precipitation**

399 All the steps were handled in an ice block at all times. The sample volume was raised to 100 uL
400 using nuclease-free water. 10 uL of 3M Sodium Acetate (Thermofisher Scientific, # R1181, USA)
401 and 300 uL of 100% EtOH were added in the sample, mixed thoroughly & incubated at -80°C
402 overnight. The next morning, samples were centrifuged at full speed (14000 rpm) for 30 minutes
403 at 4°C and supernatant was discarded. 500 uL of freshly prepared 70% EtOH was added and
404 centrifuged at full speed for 20 mins at 4°C. The supernatant was discarded and pellet was air dried
405 for 30 minutes inside the biosafety cabinet until it became transparent. Pellet was resuspended in
406 20 ul nuclease-free water and incubate at 55°C for 15 minutes to fully dissolve. The purified RNA
407 sample was stored at -80°C until further use.

408

409 Sexing of pupae

410 Kl-5 primers were used to sex individual pupae collected at the late stage [33]. PCR conditions
411 used were 95°C for 2 mins and 30 cycles of 95°C for 30 sec, 56°C for 30 sec, and 72°C for 1 min,
412 final extension of 72°C for 5 mins.

413

414 Transcriptome

415 Samples were prepared by generating a uniquely indexed library from each of the RNA samples
416 isolated from male pupae using the Illumina Stranded Total RNA Prep with RiboZero Plus
417 Microbiome kit (Illumina, USA) and custom *D. melanogaster* probes for the rRNA depletion. The
418 libraries were pooled into a single pool containing an approximately equimolar amount of the
419 samples and outsourced to the Genomic Sciences Laboratory, North Carolina State University, for
420 sequencing using NovaSeq6000 S4 150 PE lane yielding ~25 million pairs of reads per sample on
421 average. The raw reads were subjected to quality control using Trimgalore v0.6.10 with a PHRED
422 score of 20 and minimum read length of 25 bp. The cleaned reads were mapped to *D. melanogaster*
423 reference genome (v.6.12) using STAR v2.7 to generate BAM files. The read counting was
424 performed using the BAM files with featureCounts v2.0.6. The raw reads were rarefied using
425 EcolUtils v0.1 with 100 permutations setting the lowest read (16M) as the threshold. The reads
426 were then processed for downstream differentially expressed genes (DEGs) using DeSeq2 v1.42.0

427

428 Histone staining and quantification

429 Less than 8 hours old males from the same population used for HR assay above were dissected to
430 collect testes in chilled 1x PBS solution and perform histone staining as described previously [7].
431 In brief, the testes were fixed for 30 minutes at RT in 4% formaldehyde prepared in 1x PBS with
432 subsequent washing with 1x PBST solution (1x PBS + 0.3% Triton X-100) and blocking in 1%
433 BSA in PBST at RT for an hour. Samples were incubated overnight with core histone antibody
434 (MilliporeSigma, Cat#MABE71, USA) (1:1,000) at 4°C in rotating shaker. After washing with 1x
435 PBST solution (1x PBS containing 0.1% Triton X-100), samples were incubated with goat anti-
436 mouse Alexa Fluor 488 secondary antibody (Thermo Fisher Scientific, Cat#A28175, 1:500 diluted
437 in 1x PBST) in the complete dark at RT for 4 hours. After washing in 1x PBST, samples were then
438 mounted in vectashield DAPI-containing mounting media (Vector Laboratories, Cat#H-1200-10,
439 USA) for imaging using Zeiss LSM 880 confocal microscope with constant exposure settings
440 across treatment groups. The total number of late canoe-stage sperm bundles and those that
441 retained histones were quantified in each testis, and the percentage of bundles with histone
442 retention was plotted in GraphPad Prism.
443

444 Protamine staining and quantification

445 Protamine staining and quantification was evaluated using chromomycin 3 (CMA3) stain as
446 described previously [7]. In brief, mature sperm were extracted from seminal vesicles of less than
447 8 hours old males in chilled 1x PBS. Samples were fixed in 3:1 vol/vol methanol:acetic acid for
448 20 mins at 4°C. Subsequently, the slide was air-dried and treated with 0.25 mg/mL of CMA3 in
449 McIlvain's buffer, pH 7.0, with 10 mM $MgCl_2$ for 20 minutes. The samples were washed with 1x
450 PBS and mounted in vectashield DAPI-containing mounting media. Imaging was performed using
451 Zeiss LSM 880 confocal microscope. Fluorescence quantification was performed by scoring

452 fluorescent pixels in arbitrary units (A.U.) within individual sperm heads using ImageJ. The flies
453 were reared at 21°C instead of 25°C for this assay and a hatch rate was also conducted in parallel
454 to compare protamine quantification with CI induction at 21°C.
455

456 Statistical analysis

457 A comparison of data between two groups was performed using Kolmogorov-Smirnov tests and
458 a Mann-Whitney U test. For more than two groups, the Kruskal Wallis test with Benjamini, Krieger
459 & Yekutieli p-value correction was performed. A correlation test was performed using the Pearson
460 correlation coefficient. To calculate tests and plot graphs, GraphPad Prism v10.0.0 was used.
461

462 Acknowledgments

463 The authors thank the Huck Institutes Genomics Core Facility (RRID:SCR_023645) at The
464 Pennsylvania State University for generating a uniquely indexed library from each of the RNA
465 samples and custom *D. melanogaster* probes for the rRNA depletion. The co-authors also thank
466 the Microscopy Core Facility (RRID:SCR_024457) for use of the Zeiss LSM 880 confocal
467 microscope. This work was supported by The Pennsylvania State University funds to the lab of
468 SRB.
469
470

References

1. McFall-Ngai M, Hadfield MG, Bosch TCG, Carey H V., Domazet-Lošo T, Douglas AE, et al. Animals in a bacterial world, a new imperative for the life sciences. Proceedings of the National Academy of Sciences. 2013;110: 3229–3236. doi:10.1073/pnas.1218525110

2. Bordenstein SR, Theis KR. Host Biology in Light of the Microbiome: Ten Principles of Holobionts and Hologenomes. PLoS Biol. 2015;13: e1002226. doi:10.1371/journal.pbio.1002226

3. Brinker P, Fontaine MC, Beukeboom LW, Falcao Salles J. Host, Symbionts, and the Microbiome: The Missing Tripartite Interaction. Trends Microbiol. 2019;27: 480–488. doi:10.1016/j.tim.2019.02.002

4. Masson F, Lemaitre B. Growing Ungrowable Bacteria: Overview and Perspectives on Insect Symbiont Culturability. Microbiol Mol Biol Rev. 2020;84. doi:10.1128/MMBR.00089-20

5. Ludington WB, Ja WW. Drosophila as a model for the gut microbiome. PLoS Pathog. 2020;16: e1008398. doi:10.1371/journal.ppat.1008398

6. Weinert LA, Araujo-Jnr E V., Ahmed MZ, Welch JJ. The incidence of bacterial endosymbionts in terrestrial arthropods. Proceedings of the Royal Society B: Biological Sciences. 2015;282: 20150249. doi:10.1098/rspb.2015.0249

7. Kaur R, Leigh BA, Ritchie IT, Bordenstein SR. The Cif proteins from Wolbachia prophage WO modify sperm genome integrity to establish cytoplasmic incompatibility. PLoS Biol. 2022;20: e3001584. doi:10.1371/journal.pbio.3001584

8. Shropshire JD, Leigh B, Bordenstein SR. Symbiont-mediated cytoplasmic incompatibility: What have we learned in 50 years? Elife. 2020;9. doi:10.7554/eLife.61989

9. Hoffmann AA, Turelli M, Harshman LG. Factors affecting the distribution of cytoplasmic incompatibility in Drosophila simulans. Genetics. 1990;126: 933–948. doi:10.1093/genetics/126.4.933

10. Shropshire JD, Hamant E, Conner WR, Cooper BS. *cifB*- transcript levels largely explain cytoplasmic incompatibility variation across divergent *Wolbachia*. PNAS Nexus. 2022;1. doi:10.1093/pnasnexus/pgac099

11. Landmann F, Orsi GA, Loppin B, Sullivan W. Wolbachia-Mediated Cytoplasmic Incompatibility Is Associated with Impaired Histone Deposition in the Male Pronucleus. PLoS Pathog. 2009;5: e1000343. doi:10.1371/journal.ppat.1000343

12. Ingham P. The development of Drosophila melanogaster. Trends in Genetics. 1994;10: 299. doi:10.1016/0168-9525(90)90017-Z

13. Williamson A, Lehmann R. GERM CELL DEVELOPMENT IN *DROSOPHILA*. Annu Rev Cell Dev Biol. 1996;12: 365–391. doi:10.1146/annurev.cellbio.12.1.365

14. Rathke C, Baarends WM, Jayaramaiah-Raja S, Bartkuhn M, Renkawitz R, Renkawitz-Pohl R. Transition from a nucleosome-based to a protamine-based chromatin configuration during spermiogenesis in *Drosophila*. J Cell Sci. 2007;120: 1689–1700. doi:10.1242/jcs.004663

15. Akhmanova AS, Bindels PCT, Xu J, Miedema K, Kremer H, Hennig W, et al. Structure and expression of histone H3.3 genes in *Drosophila melanogaster* and *Drosophila hydei*. Genome. 1995;38: 586–600. doi:10.1139/g95-075

16. Sakaguchi A, Karachentsev D, Seth-Pasricha M, Druzhinina M, Steward R. Functional characterization of the Drosophila Hmt4-20/Suv4-20 histone methyltransferase. Genetics. 2008;179: 317–22. doi:10.1534/genetics.108.087650

17. Jayaramaiah Raja S, Renkawitz-Pohl R. Replacement by *Drosophila melanogaster* Protamines and Mst77F of Histones during Chromatin Condensation in Late Spermatids and Role of Sesame in the Removal of These Proteins from the Male Pronucleus. Mol Cell Biol. 2005;25: 6165–6177. doi:10.1128/MCB.25.14.6165-6177.2005

18. Eren-Ghiani Z, Rathke C, Theofel I, Renkawitz-Pohl R. Prtl99C Acts Together with Protamines and Safeguards Male Fertility in Drosophila. Cell Rep. 2015;13: 2327–2335. doi:10.1016/j.celrep.2015.11.023

19. Ikeda T, Ishikawa H, Sasaki T. Infection density of Wolbachia and level of cytoplasmic incompatibility in the Mediterranean flour moth, Ephestia kuehniella. J Invertebr Pathol. 2003;84: 1–5. doi:10.1016/S0022-2011(03)00106-X

20. Ritchie IT, Needles KT, Leigh BA, Kaur R, Bordenstein SR. Transgenic cytoplasmic incompatibility persists across age and temperature variation in Drosophila melanogaster. iScience. 2022;25: 105327. doi:10.1016/j.isci.2022.105327

21. Bordenstein SR, Uy JJ, Werren JH. Host Genotype Determines Cytoplasmic Incompatibility Type in the Haplodiploid Genus Nasonia. Genetics. 2003;164: 223–233. doi:10.1093/genetics/164.1.223

22. Newell PD, Douglas AE. Interspecies Interactions Determine the Impact of the Gut Microbiota on Nutrient Allocation in Drosophila melanogaster. Appl Environ Microbiol. 2014;80: 788–796. doi:10.1128/AEM.02742-13

23. Sommer AJ, Newell PD. Metabolic Basis for Mutualism between Gut Bacteria and Its Impact on the *Drosophila melanogaster* Host. Appl Environ Microbiol. 2019;85. doi:10.1128/AEM.01882-18

24. Kaur R, McGarry A, Shropshire JD, Leigh BA, Bordenstein SR. Prophage proteins alter long noncoding RNA and DNA of developing sperm to induce a paternal-effect lethality. Science (1979). 2024;383: 1111–1117. doi:10.1126/science.adk9469

25. Hughes GL, Dodson BL, Johnson RM, Murdock CC, Tsujimoto H, Suzuki Y, et al. Native microbiome impedes vertical transmission of *Wolbachia* in *Anopheles* mosquitoes. Proceedings of the National Academy of Sciences. 2014;111: 12498–12503. doi:10.1073/pnas.1408888111

26. Layton EM, On J, Perlmutter JI, Bordenstein SR, Shropshire JD. Paternal Grandmother Age Affects the Strength of *Wolbachia* -Induced Cytoplasmic Incompatibility in Drosophila melanogaster. mBio. 2019;10. doi:10.1128/mBio.01879-19

27. LePage DP, Metcalf JA, Bordenstein SR, On J, Perlmutter JI, Shropshire JD, et al. Prophage WO genes recapitulate and enhance Wolbachia-induced cytoplasmic incompatibility. Nature. 2017;543: 243–247. doi:10.1038/nature21391

28. Bourtzis K, Nirgianaki A, Markakis G, Savakis C. Wolbachia Infection and Cytoplasmic Incompatibility in Drosophila Species. Genetics. 1996;144: 1063–1073. doi:10.1093/genetics/144.3.1063

29. Cooper BS, Ginsberg PS, Turelli M, Matute DR. Wolbachia in the *Drosophila yakuba* Complex: Pervasive Frequency Variation and Weak Cytoplasmic Incompatibility, but No Apparent Effect on Reproductive Isolation. Genetics. 2017;205: 333–351. doi:10.1534/genetics.116.196238

30. Shropshire JD, On J, Layton EM, Zhou H, Bordenstein SR. One prophage WO gene rescues cytoplasmic incompatibility in *Drosophila melanogaster*. Proceedings of the National Academy of Sciences. 2018;115: 4987–4991. doi:10.1073/pnas.1800650115

31. Simhadri RK, Fast EM, Guo R, Schultz MJ, Vaisman N, Ortiz L, et al. The Gut Commensal Microbiome of Drosophila melanogaster Is Modified by the Endosymbiont *Wolbachia*. mSphere. 2017;2. doi:10.1128/mSphere.00287-17

32. Suito T, Nagao K, Juni N, Hara Y, Sokabe T, Atomi H, et al. Regulation of thermoregulatory behavior by commensal bacteria in *Drosophila*. Biosci Biotechnol Biochem. 2022;86: 1060–1070. doi:10.1093/bbb/zbac087

33. Lott SE, Villalta JE, Schroth GP, Luo S, Tonkin LA, Eisen MB. Noncanonical Compensation of Zygotic X Transcription in Early Drosophila melanogaster Development Revealed through Single-Embryo RNA-Seq. PLoS Biol. 2011;9: e1000590. doi:10.1371/journal.pbio.1000590

605

606

607 # Supporting information

608

609 **S1 Fig. Molecular confirmation of *Wolbachia* infection status of the parental lines *w*Mel-**

610 **(CV-) and *w*Mel+ (CV+).**

611

612 **S2 Fig. Conformation of microbiome absence and presence by colony forming units (CFUs)**

613 **in GF and CV lines.**

614

615 **S3 Fig. The larvae-to-pupae fitness cost in a germ-free state is neither due to *Wolbachia***

616 **density nor *cif* gene expression**.

617

618 **S1 Table: Primers used for relative quantification of Wolbachia infection check, sexing of**

619 **pupae, and quantification of cifA, cifB, and Wolbachia density**.

620

621 **S2 Table: Differentially-expressed histone, protamine, and MST genes in male pupae**.

622

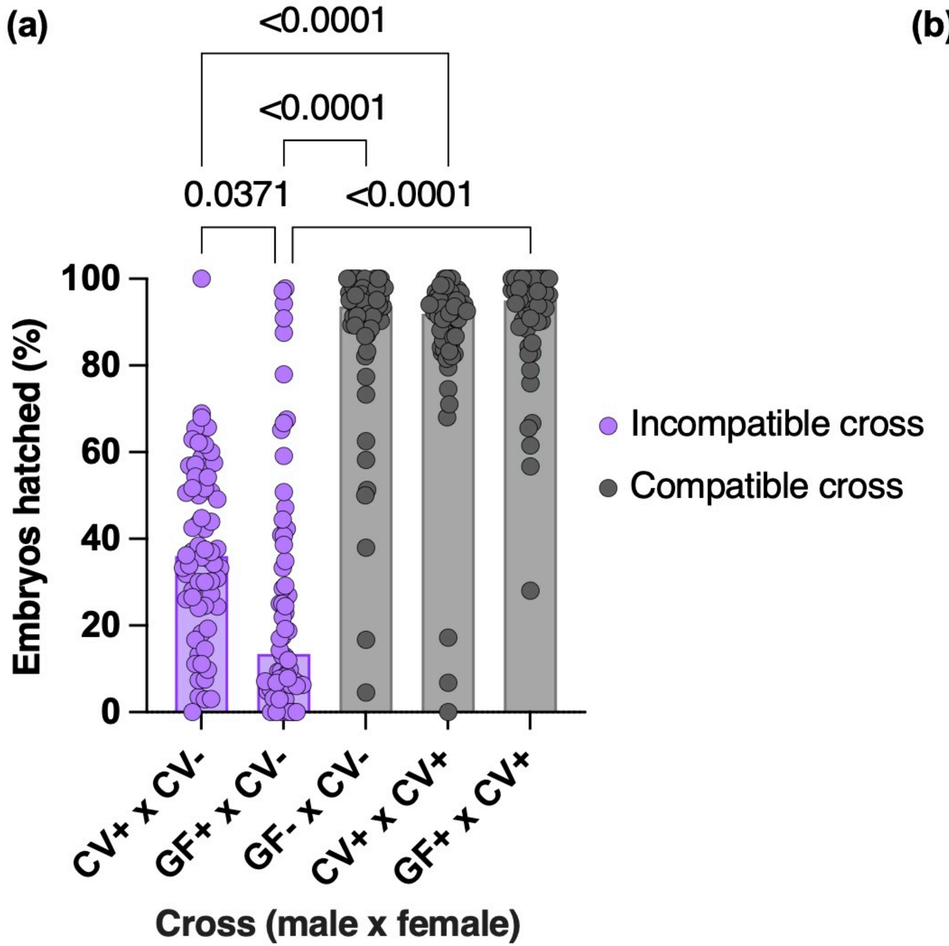
(a)
<0.0001
<0.0001
0.0371
<0.0001
Embryos hatched (%)
100
80
60
40
20
0
CV+ x CV-
GF+ x CV-
GF- x CV-
CV+ x CV+
GF+ x CV+
Cross (male x female)
Incompatible cross
Compatible cross

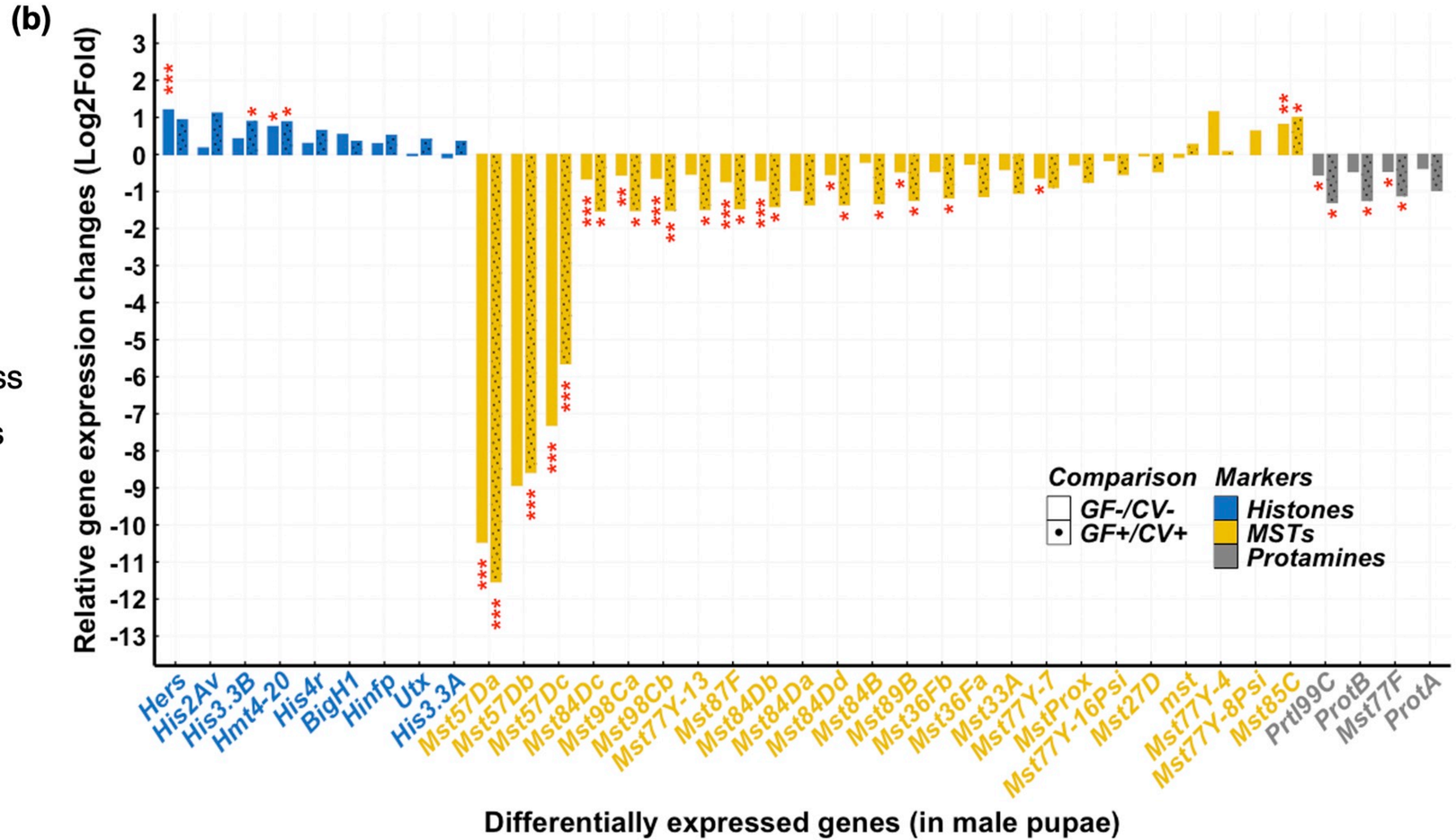
(b)
Relative gene expression changes (Log2Fold)
3
2
1
0
-1
-2
-3
-4
-5
-6
-7
-8
-9
-10
-11
-12
-13
Hers
His2Av
His3.3B
Hmt4-20
His4r
BigH1
Hinfp
Utx
His3.3A
Mst57Da
Mst57Db
Mst57Dc
Mst84Dc
Mst98Ca
Mst98Cb
Mst77Y-13
Mst87F
Mst84Db
Mst84Da
Mst84Dd
Mst84B
Mst89B
Mst36Fb
Mst36Fa
Mst33A
Mst77Y-7
MstProx
Mst77Y-16Psi
Mst27D
mst
Mst77Y-4
Mst77Y-8Psi
Mst85C
Prtl99C
ProtB
Mst77F
ProtA
Comparison
GF-/CV-
GF+/CV+
Markers
Histones
MSTs
Protamines
Differentially expressed genes (in male pupae)

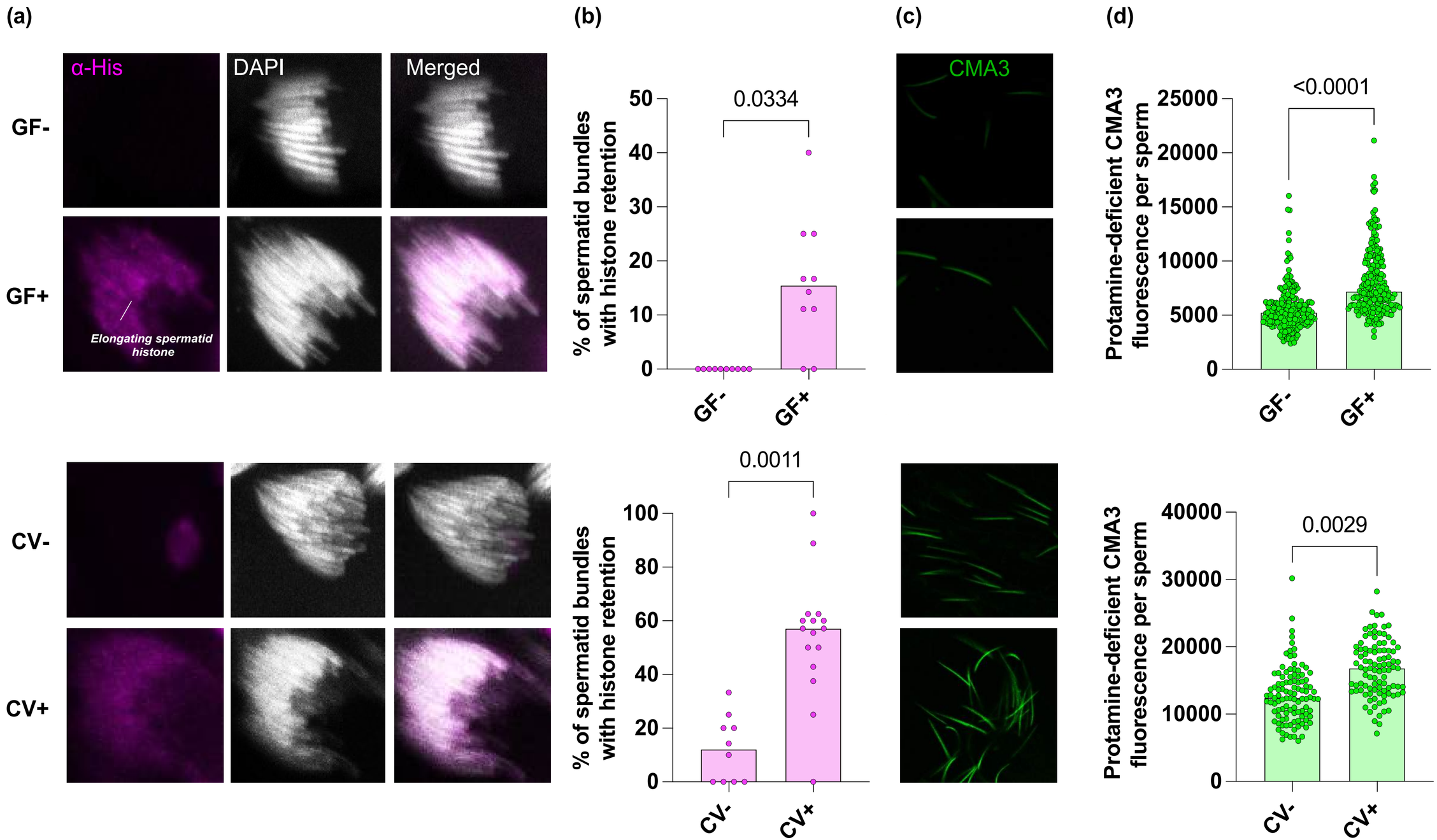
(a)
α-His
DAPI
Merged
GF-
GF+
Elongating spermatid histone
CV-
CV+
(b)
% of spermatid bundles with histone retention
0.0334
0.0011
GF-
GF+
CV-
CV+
(c)
CMA3
(d)
Protamine-deficient CMA3 fluorescence per sperm
<0.0001
0.0029
GF-
GF+
CV-
CV+

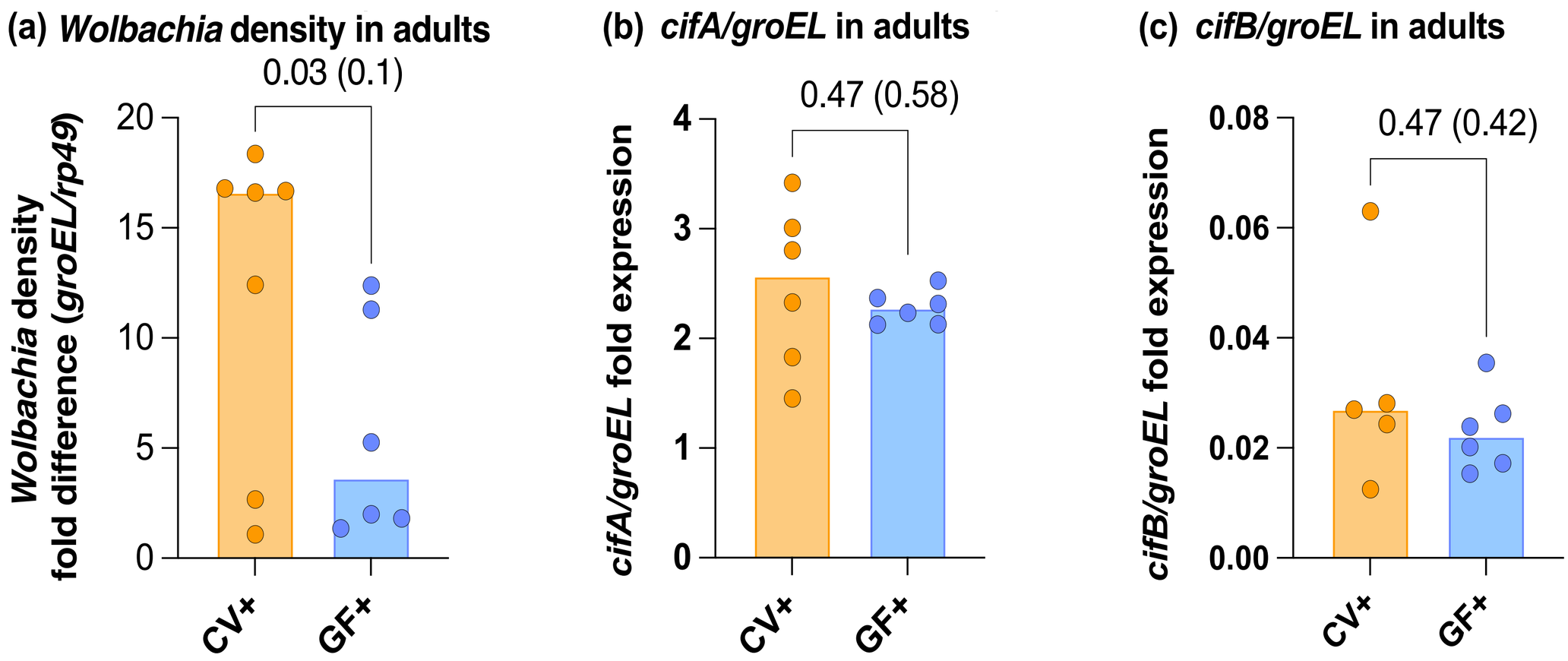
(a) Wolbachia density in adults
0.03 (0.1)
Wolbachia density
fold difference (groEL/rp49)
20
15
10
5
0
CV+
GF+
(b) cifA/groEL in adults
0.47 (0.58)
cifA/groEL fold expression
4
3
2
1
0
CV+
GF+
(c) cifB/groEL in adults
0.47 (0.42)
cifB/groEL fold expression
0.08
0.06
0.04
0.02
0.00
CV+
GF+

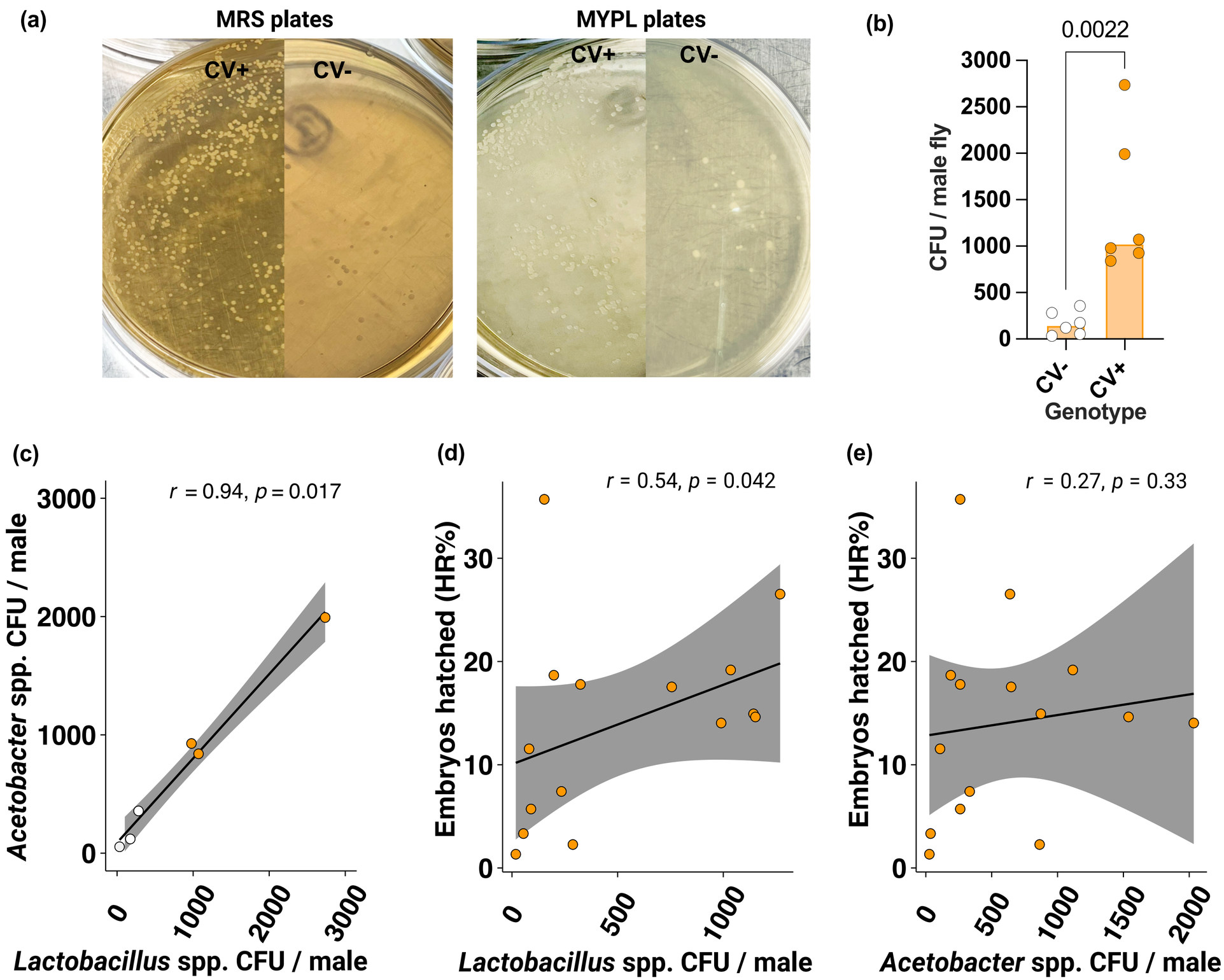
(a)
MRS plates
CV+
CV-
MYPL plates
CV+
CV-
(b)
0.0022
CFU / male fly
3000
2500
2000
1500
1000
500
0
CV-
CV+
Genotype
(c)
r = 0.94, p = 0.017
Acetobacter spp. CFU / male
3000
2000
1000
0
0
1000
2000
3000
Lactobacillus spp. CFU / male
(d)
r = 0.54, p = 0.042
Embryos hatched (HR%)
30
20
10
0
0
500
1000
Lactobacillus spp. CFU / male
(e)
r = 0.27, p = 0.33
Embryos hatched (HR%)
30
20
10
0
0
500
1000
1500
2000
Acetobacter spp. CFU / male

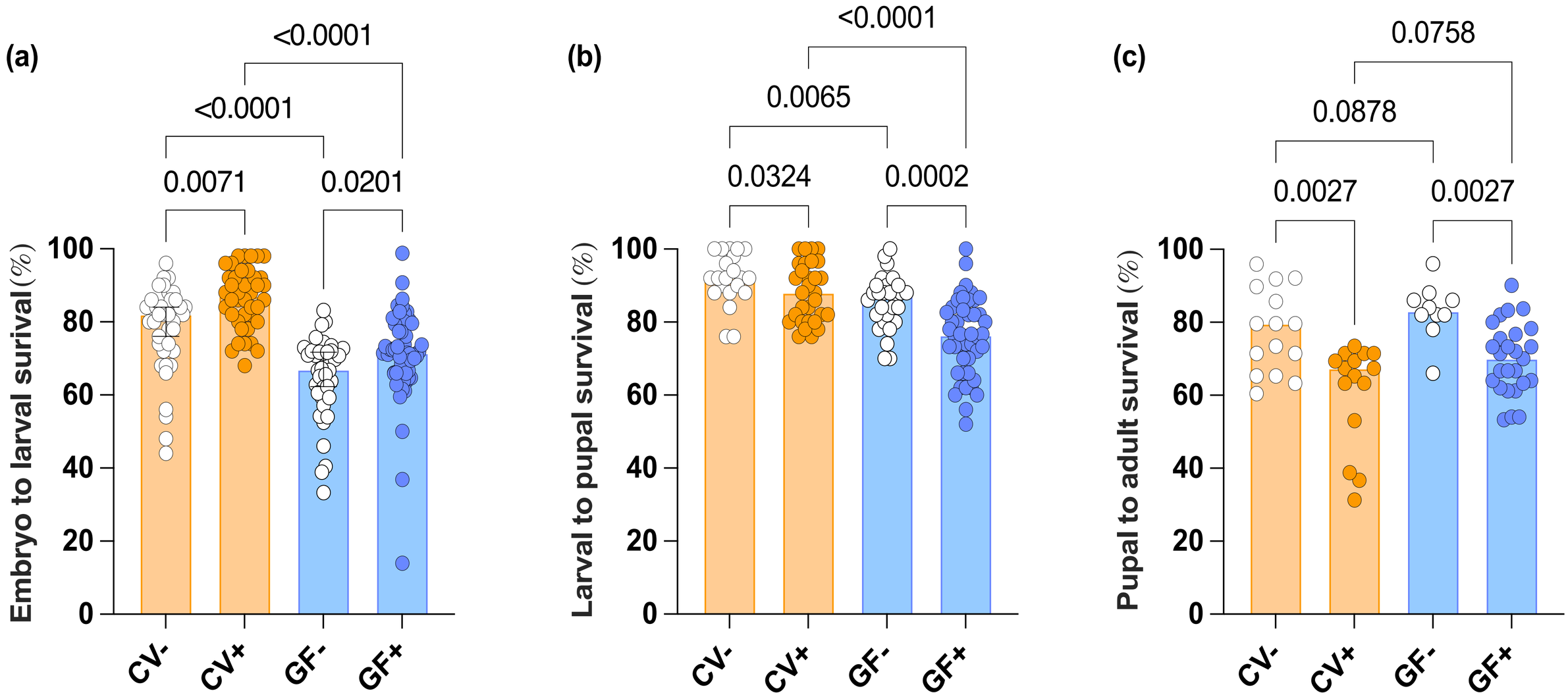
(a)
<0.0001
<0.0001
0.0071
0.0201
Embryo to larval surival (%)
100
80
60
40
20
0
CV-
CV+
GF-
GF+
(b)
<0.0001
0.0065
0.0324
0.0002
Larval to pupal survival (%)
100
80
60
40
20
0
CV-
CV+
GF-
GF+
(c)
0.0758
0.0878
0.0027
0.0027
Pupal to adult survival (%)
100
80
60
40
20
0
CV-
CV+
GF-
GF+